The Journal of Immunology

RESEARCH ARTICLE | FEBRUARY 01 2017

The MHC Class II Immunopeptidome of Lymph Nodes in Health and in Chemically Induced Colitis FREE

Tim Fugmann; ... et. al

J Immunol (2017) 198 (3): 1357–1364.
https://doi.org/10.4049/jimmunol.1601157

The MHC Class II Immunopeptidome of Lymph Nodes in Health and in Chemically Induced Colitis

Tim Fugmann,* Adriana Sofron,† Danilo Ritz,* Franziska Bootz,† and Dario Neri†

We recently described a mass spectrometry–based methodology that enables the confident identification of hundreds of peptides bound to murine MHC class II (MHCII) molecules. In this article, we describe its application to the characterization of MHCII-bound peptides isolated from lymph nodes (LNs) of C57BL/6 mice. More than 1000 peptides could be identified in individual analyses, allowing a direct comparison of the MHCII peptidome in different types of normal LNs or in animals with colitis. The peptide length distribution and consensus sequences in axillary, brachial, inguinal, and mesenteric LNs were virtually identical, and a substantial portion of identified peptides corresponded to proteins found in all LNs. However, skin-specific proteins Sbsn and Dmkn and intestine-specific proteins Dmbt1, Krt19, and Maoa, among others, were exclusively identified in skin-draining and mesenteric LNs, respectively. Differences in peptide-presentation patterns were also observed when comparing healthy mice and mice with dextran sodium sulfate–induced colitis. Peptides derived from a subset of proteins (including IgE, Bank1, chondroitin sulfate synthase 2, Cmip, and Fth1) were exclusively identified in mice with colitis, revealing changes in the peptidome associated with the inflammatory process, as well as activation and clonal expansion of B cells. ***The Journal of Immunology*****, 2017, 198: 1357–1364.**

Lymph nodes (LNs) are secondary lymphoid organs that are important for many immunological functions, including the stimulation of immune responses against pathogens and induction of peripheral tolerance (1). Migratory dendritic cells (DCs) collect Ag in surrounding tissue for presentation in draining LNs. Without additional danger signals (such as ssDNA recognized by the DC's TLR), presentation of Ags by DCs induces tolerance (2). The importance of these events can be exemplified by the observation that mice lacking $CD4^+$ $CD25^+$ regulatory T cells develop a destructive autoimmune gastritis in which $CD4^+$ T cells recognize a tissue-specific ATPase presented by DCs in gastric LNs (3). Until now, knowledge of which Ags are presented in LNs has primarily been derived from the study of model Ags (such as OVA in transgenic mice) or Ags of pathologic relevance (i.e., tumor-rejection Ags or autoantigens in model systems of autoimmunity). An alternative approach consists of the direct identification of peptides bound to MHC class II (MHCII; the MHCII peptidome) by mass spectrometry (MS). MHCII-bound peptides were first sequenced by MS 25 y ago (4). However, a comparison of the MHCII peptidomes of different cell types has been difficult because of the large number of cells (typically 1×10^9) required, essentially prohibiting the direct analysis of mouse material without further cell-expansion steps (5, 6).

Recently, we described an experimental procedure, based on the immunocapture of MHCII complexes followed by MS analysis of eluted peptides, which enabled the confident identification of thousands of MHCII-bound peptides from a hundred million murine cells or spleens (7). However, characterization of the murine MHCII peptidome from LNs, without further cultivation of isolated cells, has not been reported. As highlighted in a recent survey, "analysis of MHC class I and II peptide ligands from cells isolated in mouse primary tissue were reported with limited success given the high number of mice needed to perform an experiment" (8).

In this article, we describe an improved experimental methodology that routinely leads to the confident identification of >1000 peptides from six pooled mouse LNs, whereas only two LNs are sufficient to detect 400 peptides. A detailed comparison of LNs from healthy C57BL/6 mice revealed a high similarity in the MHCII peptidomes in axillary LNs (aLN), brachial LNs (bLNs), and inguinal LNs (iLNs). In contrast, presentation of tissue-specific proteins could be demonstrated by comparing skin-draining LNs and mesenteric LNs (mLNs). Similarly, analysis of the MHCII peptidome in healthy mice and animals with dextran sodium sulfate (DSS)-induced colitis (9) revealed differences in the corresponding peptidomes. In particular, peptides derived from Igs, Bank1, chondroitin sulfate synthase 2 (Chpf), Cmip, and Fth1 were exclusively found in mice with colitis.

Materials and Methods

Animals

iLNs, aLNs, bLNs, and mLNs were taken from three healthy C57BL/6 mice. Similarly, the three sets of six mLNs were obtained from different individual healthy C57BL/6 mice. For the induction of experimental colitis, female

*Philochem AG, CH-8112 Otelfingen, Switzerland; and †Institute of Pharmaceutical Sciences, ETH Zurich, 8093 Zurich, Switzerland

Received for publication July 5, 2016. Accepted for publication November 30, 2016.

This work was supported by the Swiss Federal Institute of Technology Zurich and by European Research Council Advanced Grant ZAUBERKUGEL (to D.N.). F.B. was supported by the Swiss National Fund and the Commission for Technology and Innovation MedTech Innitiative. A.S., D.R., T.F., and D.N. were supported by the European Union's Seventh Framework Program (FP7/2007-2013) under Grant Agreement 305309 (Profiling Responders in Antibody Therapies). D.R. and T.F. were supported by the European Union's Seventh Framework Program (FP7/2007-2013) under Grant Agreement 305608 (EURenOmics).

D.N. and T.F. conceived, designed, and supervised the study and wrote, reviewed, and/or revised the manuscript; A.S., D.R., and F.B. developed the methodology; A.S., D.R., and T.F. acquired data; and T.F. analyzed and interpreted the data.

Address correspondence and reprint requests to Prof. Dario Neri or Dr. Tim Fugmann, Institute of Pharmaceutical Sciences, ETH Zurich, Vladimir-Prelog-Weg 1-5/10, HCI G 392.4, 8093 Zurich, Switzerland (D.N.) or Philochem AG, Libernstrasse 3, CH-8112 Otelfingen, Switzerland (T.F.). E-mail addresses: dario.neri@pharma.ethz.ch (D.N.) or tim.fugmann@philochem.ch (T.F.)

The online version of this article contains supplemental material.

Abbreviations used in this article: aLN, axillary LN; bLN, brachial LN; Chpf, chondroitin sulfate synthase 2; DC, dendritic cell; DSS, dextran sodium sulfate; FDR, false discovery rate; iLN, inguinal LN; LN, lymph node; MHCII, MHC class II; mLN, mesenteric LN; MS, mass spectrometry; m/z, mass-to-charge ratio; PSSM, position-specific scoring matrix; ROC, receiver operating characteristic.

SOPF C57BL/6 mice were purchased from Janvier Labs (Laval, France). All experiments described in this article were performed under the project license Dextran Sodium Sulfate (DSS)-Induced Colitis Mouse Model for Diagnostics and Therapy (Bew. Nr. 26/2013) issued to D.N. by the local cantonal authority (Veterinäramt des Kantons Zürich).

Induction of experimental colitis in mice

Induction, monitoring, and collection of samples from mice with DSS colitis were performed as described (9). Briefly, 8-wk-old mice were administered 2.5 to 3.0% (w/v) DSS (40,000 g/mol; TdB Consultancy) in drinking water for five consecutive days ad libitum. Thereafter, mice received water plus 5% glucose and 0.25% $NaHCO_3$ for an additional 7 d. From day 12, mice received normal drinking water. At day 25, mice with colitis were sacrificed, and mLNs were collected. LNs were collected from healthy animals upon sacrifice at 12 wk of age.

Affinity purification of MHCII complexes and peptides

The purification of MHCII complexes from tissue lysates was essentially performed as described (7). Because of the enlargement of mLNs in animals with chemically induced colitis and the variation in the weights of these LNs, 20–25 mg of total tissue was pooled for the analysis of inflamed LNs, corresponding to one to two LNs. In brief, LNs were disrupted with a tissue lyser (QIAGEN) for 2 min at 25 Hz in lysis buffer (0.5% deoxycholate, 1% IGEPAL CA-630, 50 mM Tris, 150 mM NaCl, 0.1% SDS, 0.2 mM iodoacetamide, 1 mM EDTA, and 1 mM PMSF; Roche Complete Protease Inhibitor Cocktail [pH 7.4]). MHCII complexes were purified from tissue lysates with M5/114 Ab coupled to solid support. After a 2-h incubation at 4˚C, unbound protein was removed by washing with 10 ml of lysis buffer, 10 ml of buffer A (150 mM NaCl, 20 mM Tris-HCl [pH 7.4]), 10 ml of buffer B (400 mM NaCl, 20 mM Tris-HCl [pH 7.4]), 10 ml of buffer A, and 10 ml of buffer C (20 mM Tris-HCl [pH 8]). MHCII complexes were eluted after the last wash in 1 ml of 10% acetic acid. Eluates were subjected to C18 purification using Macro SpinColumns (Harvard Apparatus). Peptides were eluted in 25% acetonitrile, 0.1% trifluoroacetic acid and dried with a vacuum concentrator (Christ Alpha RVC). The dried peptides were stored at −20˚C until MS analysis.

Analysis of MHCII peptides by liquid chromatography–coupled MS

Peptides were analyzed with a Q Exactive Hybrid Quadrupole-Orbitrap Mass Spectrometer coupled to an EASY-nLC 1000 (both from Thermo Fisher). The peptides were resolved using an Acclaim PepMap RSLC analytical column (Thermo Fisher) with a linear gradient from 0 to 20% acetonitrile in 45 min. All buffers contained 0.1% formic acid. Spectra were collected in the Orbitrap mass analyzer using full-ion scan mode over the mass-to-charge ratio (m/z) range 380–2000, with a resolution of 70,000 at 200 m/z with a maximum injection time of 80 ms and a tandem MS resolution of 17,500 at 200 m/z with a maximum injection time of 240 ms. The 10 most intense masses from each full mass spectrum were selected for fragmentation by higher-energy collisional dissociation in the C-trap. Spectra were processed with Proteome Discoverer (Version 1.4.1.14; Thermo Scientific) and searched with SEQUEST against a database consisting of the murine reference proteome (52,639 entries) downloaded from the UniProt homepage on January 20, 2015 or a database consisting of the murine reference proteome (52,639 entries) concatenated with bacterial proteins of UniProt proteome IDs UP000012594, UP000012542, UP000027129, UP000013570, UP000017429, UP000012445,

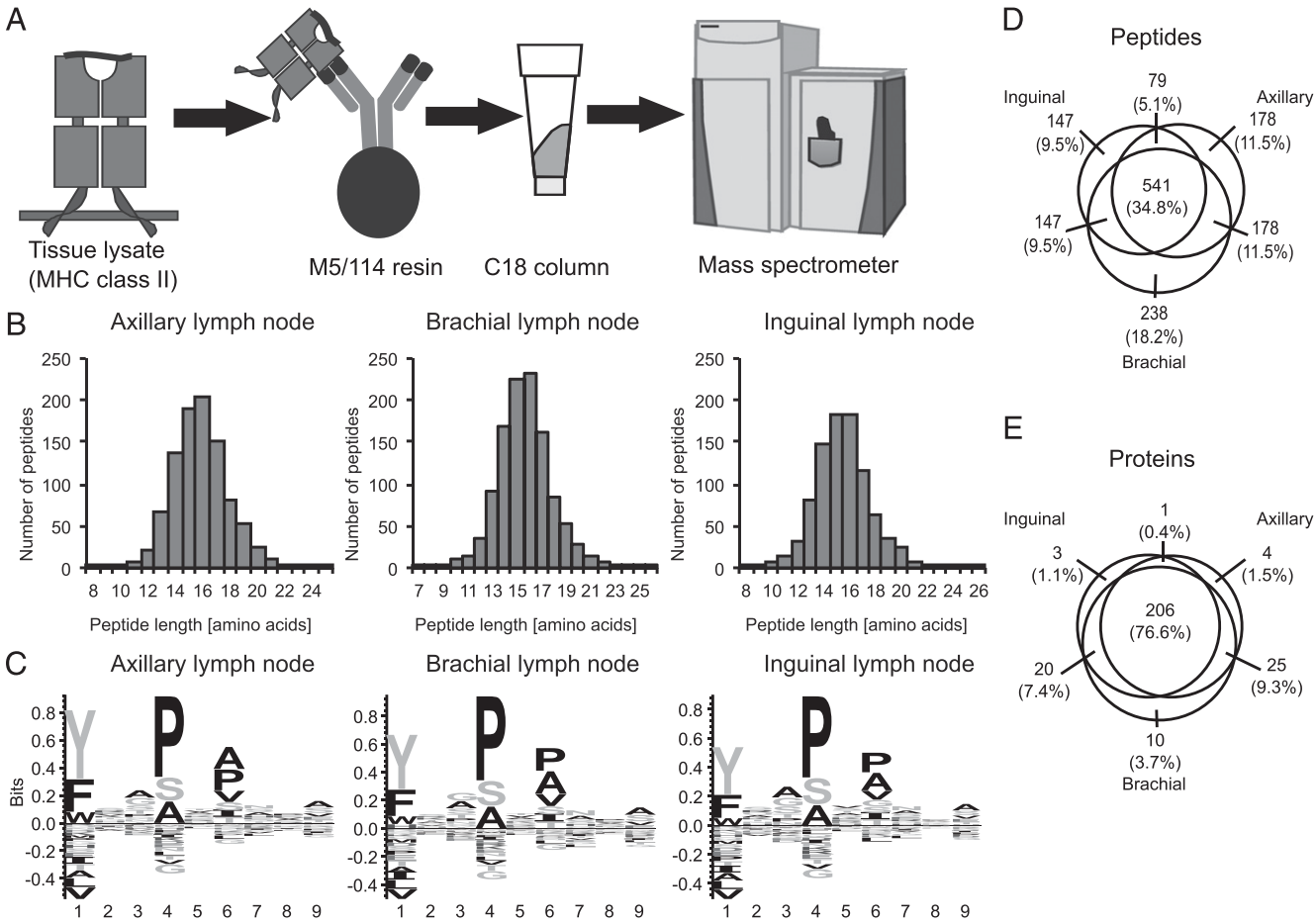

FIGURE 1. Characterization of the MHCII peptidome from skin-draining LNs from different anatomical locations. (**A**) General schema for the isolation of MHCII complexes and purification of eluted peptides. MHCII complexes are purified from LN lysates with anti-murine MHCII Ab M5/114-resin. After elution of the MHCII-bound peptides with 10% acetic acid, peptides are desalted with C18 resin and analyzed by liquid chromatography–coupled MS. (**B**) Length distribution of peptides identified from the lysate of pools of six aLNs, bLNs, and iLNs. (**C**) Consensus sequences of eluted MHCII peptides of aLNs, bLNs, and iLNs, as identified with the GibbsCluster 1.0 server (11) and visualized with Seq2Logo 2.0 (12). Peptides (**D**) and proteins with at least two peptides in total (**E**) identified from aLNs, bLNs, and iLNs. Circles are drawn proportional to the size of the peptidomes and to the overlap between the samples, but they only approximate the overlap between proteins.

UP000012582, and UP000012589 corresponding to the following bacterial strains: *Lactobacillus* sp. ASF360, *Lactobacillus murinus* ASF361, *Lactobacillus animalis*, *Parabacteroides* sp. ASF519, *Mucispirillum schaedleri* ASF457, *Clostridium* sp. ASF356, *Clostridium* sp. ASF502, and *Eubacterium plexicaudatum* ASF492. The 31,960 total protein entries of the eight proteomes were downloaded from the UniProt homepage on March 21, 2016. Furthermore, the following analysis settings were used for the identification of peptides and proteins: no-enzyme (unspecific), precursor mass tolerance 4 ppm, fragment mass tolerance 0.02 Da, one variable modification (oxidation of methionine), and percolator peptide validation 1% false discovery rate (FDR). Peptide to protein annotation was performed with DeepQuanTR software (10). All peptides were annotated to mouse or bacterial origin. To ensure high-confidence identification, peptides were filtered for a length of 9–25 aa, typically found for MHCII peptides. Further, peptides with an XCorr value < 2 were discarded, because these typically derive from spectra with few informative fragments. However, a manual BLAST search was performed for all bacterial high-confidence identifications to rule out the probability of ambiguous annotation resulting from isoleucine–leucine substitutions. No homologous rodent sequences were reported for the five bacterial peptides.

For the identification of MHCII-specific motifs, peptides were aligned with the GibbsCluster-1.0 Server (11) using the default settings, with the exception of the motif length, which was set to 9 aa. A trash cluster was used to remove outliers, keeping the threshold for discarding to trash at zero. MHCII-specific motifs were visualized after Gibbs clustering with the Seq2Logo 2.0 server (12).

Gene expression profiling

The mouse mRNA expression dataset GeneAtlas MOE430, gcrma (13), accessible through BioGPS (14), was interrogated for expression data of the 20 genes identified exclusively in intestine or skin (Table I). Data from probes demonstrating an SD < 5 over all analyzed samples were ignored to remove transcripts with very low signal-to-noise. Remaining expression data for all probes in epidermis and intestine (including small and large intestine) were averaged, and the ratio between epidermis and intestine was calculated.

Matrix-based scoring of peptide sequences and peptide–MHCII binding prediction

Our previous data (7) were used for the calculation of position-specific scoring matrices (PSSMs). Peptide sequences identified from spleens of BALB/c or C57BL/6 mice were submitted to GibbsCluster-1.1 server (11) analysis using the standard parameters, with the exception of the motif length (set to 9 aa) and the use of a trash cluster. Core sequences identified from the clustering analysis of the I-A^d or I-A^b cluster were submitted to the Seq2Logo 2.0 server (12), using the following parameters: logo type, Kullback-Leibler; clustering method, Hobohm1; threshold for clustering, 0.63; weight on prior, 200; information content, bits. In the advanced settings, Blossum62 matrix and respective background frequencies were enabled. From the resulting logo, the corresponding PSSM was downloaded and used for all scorings (Supplemental Fig. 1A, 1B). Scoring was performed by applying a sliding window of 9 aa to each peptide sequence, saving the highest score for each peptide, assuming that this is the most likely MHCII-binding region. For the false-positive dataset, we assumed that the majority of sequences of the mouse proteome are not binding to a given MHCII allele. This assumption is supported by the fact that we only observe peptide sequences around 1–10 central core sequences for any protein. Therefore, all theoretical 15mer sequences of the murine reference proteome (52,639 protein entries) downloaded from the UniProt homepage on January 20, 2015 were calculated and scored using the PSSM-based scoring function. True-positive data (the scores for peptides eluted from BALB/c or C57BL/6 spleens) and false-positive data (the scores of the 15mer sequences from the murine reference proteome) were subjected to a receiver operating characteristic (ROC) curve analysis, and the cut-off value (for which the distance to the diagonal [i.e., the random distribution] is largest) deduced from the ROC curve was defined as the minimum score to predict binding to the respective MHCII alleles.

Prediction of peptide–MHCII binding with the NetMHCIIpan 3.1 Server (15) was performed, keeping all standard parameters, selecting the MHCII allele I-A^d or I-A^b and submitting peptide sequences with ≥ 9 aa. The threshold for binding was defined as a rank $< 10\%$.

Results

MHCII peptidome analysis of murine LNs

We applied a refined procedure for the analysis of MHCII-bound peptides depicted in Fig. 1A. MHCII complexes were purified from tissue homogenates using the M5/114 Ab (16) coupled to a solid support. After stringent washing, peptides were eluted in acid and purified by applying a single C18 purification step. Compared with ultrafiltration, this single step after elution was crucial for improved recovery of peptides, still efficiently separating peptides from proteins (7). Eluted peptides were analyzed by liquid chromatography–coupled MS, applying a stringent FDR ($<1\%$) during the database search. This procedure led to an optimal balance between the total number of peptide identifications and the fraction of predicted MHCII binders (Supplemental Fig. 1C, 1D).

Using this method, we analyzed single LNs, as well as pools of two, four, and six LNs, from healthy C57BL/6 animals in an effort to determine the feasibility of the MHCII peptidome analysis of such a limited amount of sample. Peptide identifications increased from an average of 137 to 1034 when moving from one to six LNs, respectively. Throughout this study, we pooled six healthy LNs because the quantity of identified peptides was relatively large for the limited amount of sample, and it allowed us to keep the number of animals required for the analyses at a minimum.

The analysis of three pools of six LNs, derived from three C57BL/6 mice, provided a high level of reproducibility (Fig. 1C–E, Supplemental Table I), with a total of 976, 1149, and 914 peptides

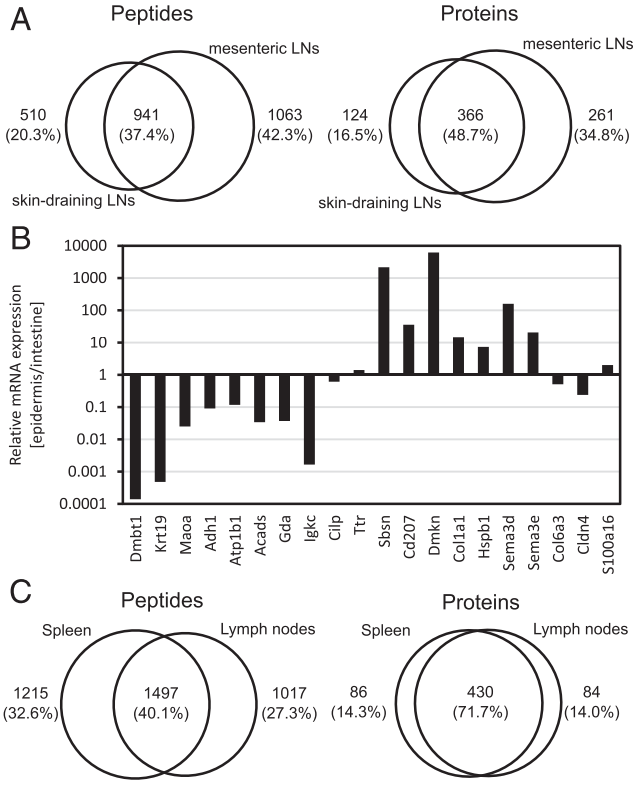

FIGURE 2. Comparative analysis of the MHCII peptidomes isolated from aLNs, bLNs, iLNs, mLNs, and spleen. (**A**) Peptides (left panel) and proteins with at least two peptides in total (right panel) identified from skin-draining LNs and mLNs. Circles are drawn proportional to the size of the peptidomes and to the overlap between the samples. (**B**) Relative mRNA expression of the proteins presented exclusively in skin-draining LNs or mLNs (Table I). Epidermal and intestinal mRNA expression was retrieved with BioGPS (14) averaged over all transcripts and all samples. (**C**) Peptides (left panel) and proteins with at least two peptides in total (right panel) identified from aLNs, bLNs, iLNs, and mLNs compared with spleen. Spleen data were reported previously (7). Circles are drawn proportional to the size of the peptidomes and to the overlap between the samples.

identified from iLNs, aLNs, and bLNs, respectively, with an average length of 15–16 aa (Fig. 1B). The peptide consensus motifs for all samples were virtually identical (Fig. 1C) and revealed the I-A^b–specific motif, in agreement with previous reports (7, 17). Between 62 and 66% of the peptides with a length $\geq$ 15 aa identified in the four LN sets were predicted to bind to I-A^b by NN-align (18). Although 541 peptides (34.8% of all identified peptides) were shared between aLNs, bLNs, and iLNs, 206 source proteins with two or more peptides (76.6%) were shared among all samples, indicating that the peptidomes of these LNs are very similar (Fig. 1D, 1E). The observation that the peptidome of aLNs, bLNs, and iLNs is very similar is not surprising, because they drain similar tissues. At this stage, it is difficult to confidently identify any significant difference between different anatomical locations. Therefore, in the following section, these LNs are collectively referred to as skin-draining LNs.

Comparison of the LN MHCII peptidome between different anatomical locations

Having established the technical reproducibility of the methodology, we asked whether the MHCII peptidomes of different LNs would correspond to similar sets of peptides and proteins. Therefore, we collected and analyzed a triplicate set of pools of six mLNs from C57BL/6 mice. Pairwise comparisons of peptide sets identified in these LNs revealed an overlap of 48.0–70.5% on the protein level. The combined mLN peptidome, resulting from the three pools, was compared with the corresponding skin-draining LN peptidome. In this case, 48.7% of the source proteins were shared, whereas 16.5 and 34.8% were exclusively identified in skin-draining LNs and mLNs, respectively (Fig. 2A).

To learn about differences in peptide presentation on MHCII from skin-draining LNs and mLNs, we decided to focus on the most striking differences between the two data sets. Proteins identified with the highest number of peptides are listed in Table I and primarily corresponded to proteins of the peptide-presentation machinery (MHCII α-chain and CLIP), the BCR (Cd79a), and several serum components (e.g., Apoe, Alb, and Mug1). For example, the 38 individual peptide sequences identified from MHCII α-chain centered around three core sequences containing signatures of the I-A^b binding motif. This observation indicates that the majority of peptides identified in this study had been eluted from MHCII and were not process-related contaminants (Supplemental Table I).

Cd207, a marker of epidermal Langerhans cells, was exclusively identified in aLNs, bLNs, and iLNs. A similar observation was made for Sbsn and Dmkn, two proteins with specific expression in skin (Fig. 2B, Table I). Moreover, Col1a1, Hspb1, Sema3d, and Sema3e were found to have higher expression in the epidermis than in the intestine (Fig. 2B). In contrast, peptide identification in mLNs revealed Dmbt1, Krt19, Maoa, Aldh1, Atp1b1, Acads, Gda,

Table I. Selection of proteins for which at least two peptides were identified in healthy aLNs, bLNs, iLNs, and mLNs

UniProt Accession No.	Protein Name	Gene Name	iLN	aLN	bLN	mLN 1	mLN 2	mLN 3	Peptides Skin-Draining LNs	Peptides mLNs
P04441	H-2 class II histocompatibility Ag γ-chain	Cd74	16	28	21	50	15	18	32	52
A0A075B5P6	Ig μ chain C region	Ighm	19	24	19	52	21	20	25	52
P14483	H-2 class II histocompatibility Ag, A β-chain	H2-Ab1	27	30	26	38	20	22	33	38
O88307	Sortilin-related receptor	Sorl1	12	19	15	34	8	6	22	35
P13020	Gelsolin	Gsn	16	24	15	17	3	4	29	17
P08226	Apolipoprotein E	Apoe	25	25	22	28	17	16	27	29
P11911	B cell Ag receptor complex-associated protein α-chain	Cd79a	20	25	20	27	20	18	25	28
P07724	Serum albumin	Alb	19	21	18	25	11	10	24	25
Q62312	TGF-β receptor type-2	Tgfbr2	7	9	5	19	6	11	13	26
P28665	Murinoglobulin-1	Mug1	16	17	10	22	16	10	19	24
E9QPG8	Deleted in malignant brain tumors 1 protein	Dmbt1				12	6	7	0	14
P19001	Keratin, type I cytoskeletal 19	Krt19				11	3	3	0	11
Q64133	Amine oxidase (flavin-containing) A	Maoa				6	6	5	0	7
P00329	Alcohol dehydrogenase 1	Adh1				5	3	2	0	5
P14094	Sodium/potassium-transporting ATPase subunit β-1	Atp1b1				5	1	1	0	5
Q07417	Short-chain specific acyl-CoA dehydrogenase, mitochondrial	Acads				3	1	1	0	3
Q9R111	Guanine deaminase	Gda				3	2	2	0	3
P01634	Ig κ-chain V-V region MOPC 21	n/a				1	2	1	0	2
Q66K08	Cartilage intermediate layer protein 1	Cilp				1	2	1	0	2
P07309	Transthyretin	Ttr				1	1	1	0	2
E9QPB2	Suprabasin	Sbsn	14	12	9				15	0
Q8VBX4	C-type lectin domain family 4 member K	Cd207	13	12	13				14	0
E9Q2P1	Dermokine	Dmkn	11	10	7				13	0
P11087	Collagen α-1(I) chain	Col1a1	6	4	8				8	0
P14602	Heat shock protein β-1	Hspb1	3	3	7				7	0
Q8BH34	Semaphorin-3D	Sema3d	6	4	3				7	0
P70275	Semaphorin-3E	Sema3e	4	5	6				6	0
E9PWQ3	Protein Col6a3	Col6a3	3	4	3				5	0
O35054	Claudin-4	Cldn4	4	3	4				5	0
Q9D708	Protein S100a16	S100a16	3	4	2				5	0

and Igkc. The corresponding genes were preferentially expressed in the intestine (Fig. 2B, Table I). A comparison of the MHC peptidomes of LNs and spleens revealed that the tissue-specific proteins, such as Dmbt1, Cd207, Sbsn, or Dmkn, were also not present in spleens. Interestingly, although more peptides were identified from C57BL/6 spleens, a total of 1017 peptides and 84 proteins with at least two peptides were exclusively found in LN samples (Fig. 2C).

Consensus motifs and scoring function

Analysis of the peptidomes derived from BALB/c and C57BL/6 spleens (the training data sets) allowed the definition of consensus motifs and of scoring functions that could be used for the interrogation of additional biological specimens (Fig. 3A).

To define a score threshold discriminating between binders and nonbinders, true positives (i.e., peptides eluted from spleen) and false positives (i.e., all possible 15mer sequences of the murine reference proteome) were subjected to an ROC curve analysis to define the cut-off point for which the distance to the diagonal (i.e., the random distribution) is largest (Fig. 3B).

The scoring function and the score threshold, obtained from this training set of peptide identifications, allowed a better description of potential binders compared with NetMHCIIpan 3.1 (15) in a validation data set, based on the peptidome of A20 cells (derived from BALB/c mice) and C57BL/6 LNs (Fig. 3C).

Analysis of mLN MHCII peptidome during experimental colitis

We further applied the methodology to study MHCII peptidome changes during DSS-induced colitis, a model routinely used to chemically induce a condition that mimics human ulcerative colitis (19). In total, two sets of normal mLNs were compared with five pools of inflamed LNs 25 d after induction of colitis. Again, the MHCII peptidome of animals with colitis was reproducible, with 223 proteins (63.5%) with at least two peptide sequences identified in all five samples (Supplemental Table II).

Prominent proteins identified exclusively or with significantly more peptides from inflamed LNs include Igs, such as IgA (Igha) and IgE (Ig ε chain C region), Bank1, Chpf, Cmip, Fth1, Slamf6, Tlr9, Itgb7, and Notch3 (Table II).

Identification of bacterial Ags from mLNs

The intestinal immune system maintains a delicate balance between defense against pathogens and tolerance to commensal bacteria (20). Essential for both processes are DC subsets, which present peptides from pathogenic and commensal bacteria on MHCII in mLNs, thereby initiating an adaptive immune response or inducing tolerance (21). However, an aberrant immune response against commensal bacteria may eventually lead to chronic colitis (20).

We probed the MS data for eight bacterial strains contained in the altered Schaedler flora, which are widely used to inoculate germ-free founder animal breeding colonies (22), by performing a separate database search with SEQUEST. Bacterial peptide identifications were additionally filtered for XCorr > 2 (length of 9–25 aa) and compared with rodent proteomes using BLAST, to verify that these identifications were not false positives resulting from homologous murine proteins. After these stringent filtering criteria, only five peptides identified from healthy or inflamed mLNs could be unambiguously annotated to bacterial proteins, including one from *Clostridium* sp. ASF502, three from *E. plexicaudatum* ASF492, and one from *Parabacteroides* sp. ASF519 (Table III, Supplemental Table III). Of the five peptides, the three longer ones had elements of I-A^b binding motifs (underlined in Table III). Although none of the five peptides was predicted to bind to I-A^b

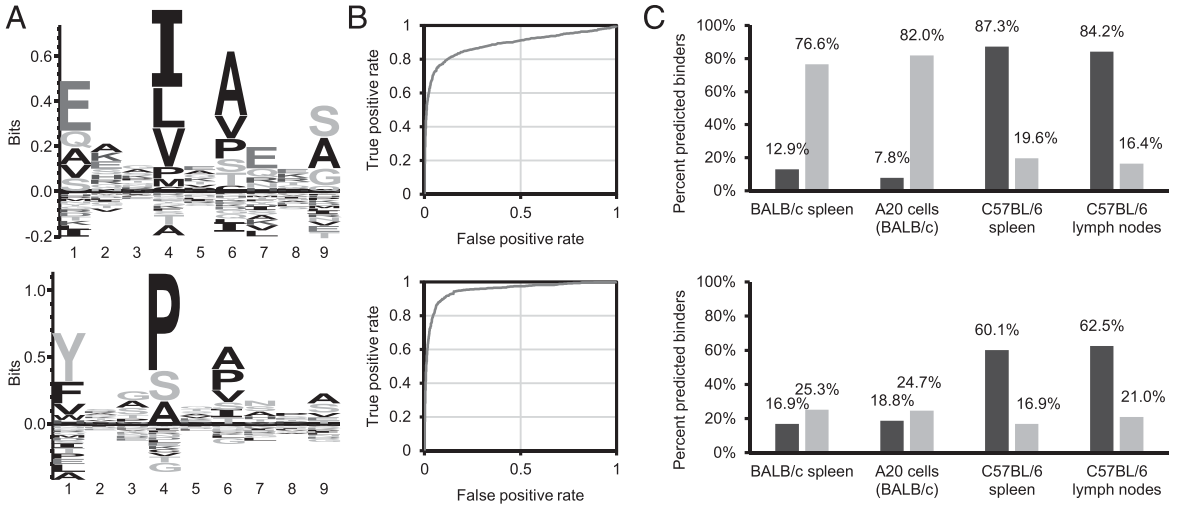

FIGURE 3. Matrix-based prediction of the binding of peptide sequences to mouse MHCII alleles I-A^b and I-A^d. (**A**) MHC-specific motif of I-A^d (upper panel) and I-A^b (lower panel). For the creation of the motifs, I-A^d and I-A^b complexes were purified from BALB/c or C57BL/6 spleens, respectively, and eluted peptides were analyzed by MS. Peptide sequences identified with 1% FDR were clustered with GibbsCluster-1.1 server (11), and resulting I-A^d– and I-A^b–specific motifs were visualized with Seq2Logo 2.0 (12). Seq2Logo also provides PSSMs (Supplemental Fig. 1A, 1B), which are the basis to calculate scores. (**B**) ROC curves showing the performance of the matrix-based scoring to discriminate between a true positive set (i.e., peptide sequences eluted from I-A^d [upper panel] or I-A^b [lower panel]) and a false positive set (i.e., all 15mer sequences derived from the murine reference proteome). The point at which the distance to the diagonal (i.e., the random distribution) is largest was defined as the score cut-off predicting binding to respective MHCII alleles. According to this definition, the minimum score to predict binding was 8.0 for I-A^d and 8.5 for I-A^b. (**C**) Evaluation of the matrix-based scoring (upper panel) and NetMHCIIpan 3.1 (lower panel) (15) to predict binding of peptide sequences eluted from MHCII complexes to their cognate MHCII alleles. Peptide sequences eluted from BALB/c or C57BL/6 spleens represent the training datasets used to compute the PSSM and the minimum score to predict binding. Peptide sequences from MHCII complexes of A20 cells (a B cell lymphoma cell line derived from BALB/c mice) and C57BL/6 LNs represent validation data. Binding was predicted by interrogating the peptide sequences for binding to I-A^d (light gray) or to I-A^b (dark gray) with the respective PSSMs or by selecting the respective allele on the NetMHCIIpan 3.1 server Web site. Peptide sequences identified from A20 cells and BALB/c and C57BL/6 spleens were taken from Sofron et al. (7).

Table II. Selection of proteins identified in healthy or inflamed mLNs and corresponding number of peptides

UniProt Accession No.	Protein Name	Gene Name	M1[a]	M2[a]	C1[b]	C2[b]	C3[b]	C4[b]	C5[b]
P14483	H-2 class II histocompatibility Ag, A β-chain	H2-Ab1	31	36	34	36	38	38	35
A0A075B5P6	Ig μ chain C region	Ighm	21	32	28	35	36	33	37
P08226	Apolipoprotein E	Apoe	24	23	23	29	30	25	26
P11911	B cell Ag receptor complex-associated protein α-chain	Cd79a	19	25	24	26	25	27	23
P04441	H-2 class II histocompatibility Ag γ-chain	Cd74	14	24	21	29	29	20	16
O88307	Sortilin-related receptor	Sorl1	16	15	17	25	28	24	21
P07724	Serum albumin	Alb	21	22	12	18	18	16	19
Q62312	TGF-β receptor type-2	Tgfbr2	13	18	13	17	20	20	17
P28665	Murinoglobulin-1	Mug1	9	14	8	14	13	11	13
O09126	Semaphorin-4D	Sema4d	10	13	11	12	12	12	12
A0A075B6A3	Protein Igha	Igha	4	7	8	11	10	5	5
A0A075B5P4	Ig γ-1 chain C region secreted form	Ighg1	3	3	3	9	11	2	3
P06336	Ig ε chain C region	n/a			2	3	6		1
Q80VH0	B cell scaffold protein with ankyrin repeats	Bank1			2	2	4	3	1
D6RFA4	Chondroitin sulfate synthase 2	Chpf			1	2	2	2	2
A0A075B5M2	Protein Igkv4-61	Igkv4-61				2	2	1	2
Q9D486	C-Maf-inducing protein	Cmip				2	3	1	1
P09528	Ferritin H chain	Fth1				1	2	2	1
P18527	IgH V region 914	n/a			2	1	1	1	1
P05366	Serum amyloid A-1 protein	Saa1				2	2	1	1
Q9ET39	SLAM family member 6	Slamf6				2	3		1
Q8BZQ2	Cysteine-rich secretory protein LCCL domain-containing 2	Crispld2				1	2	2	
D3YUE2	Procollagen C-endopeptidase enhancer 1	Pcolce			1	1	1		2
P50446	Keratin, type II cytoskeletal 6A	Krt6a			2	2		1	
P62774	Myotrophin	Mtpn				2	2		1
Q3UV17	Keratin, type II cytoskeletal 2 oral	Krt76				3	2		
Q9EQU3	TLR 9	Tlr9			1	1	1	1	1
P26011	Integrin β-7	Itgb7			1	1	1	1	1
Q61982	Neurogenic locus notch homolog protein 3	Notch3			1	1	1	1	1
E9PZW0	Desmoplakin	Dsp	5						
M9MMK0	Semaphorin-3B	Sema3b	2	2					
P61164	α-centractin	Actr1a	1	2					
O08852	Polycystin-1	Pkd1		2					
Q8R016	Bleomycin hydrolase	Blmh	2						
F6YSS8	Intelectin-1a (Fragment)	Itln1	1	1					
Q5U462	CUB domain-containing protein 1	Cdcp1	1	1					
P49138	MAPK-activated protein kinase 2	Mapkapk2	1	1					
Q99PG0	Arylacetamide deacetylase	Aadac	1	1					
Q80T21	ADAMTS-like protein 4	Adamtsl4	1	1					

[a]M1–M2, mLNs from healthy mice.
[b]C1–C5, inflamed mLNs from mice with experimental colitis.

by the matrix-based scoring (a score > 8.5 indicates binding to I-A^b, Fig. 3), one of the peptides had a score of 7.2 and may represent a potential binder. The corresponding source protein represents an uncharacterized protein predicted to bind to DNA, because it contains an OmpR/PhoB-type DNA-binding domain. Interestingly, the proteins with accession N1ZXV2 and N2A3Y1 with unknown function both contained DUF4874 and DUF4832 domains.

Discussion

In this article, we report the refinement and application of a highly sensitive MHCII peptidome analysis (7) to the study of limited numbers of healthy and inflamed LNs. Initial observations suggested that the homogenization of six healthy skin-draining LNs pooled from the same mouse with a bead mill results in reproducible MHCII peptidomes, with an acceptable number of peptide identifications (~1000, Fig. 1). It is possible that other lysis methods, such as Micro Pestle–assisted pressure cycling technology, applicable to the lysis of 1–2 mg of tissue (23) could yield acceptable numbers of peptides from single LNs. However, it needs to be proved that the reproducibility can be improved over the bead mill and that the MHCII complex remains intact during this procedure.

The MHCII peptidomes of iLNs, aLNs, and bLNs demonstrated that they are comparable, with 67.4% of proteins with two or more peptides identified in all LN samples. Similar levels of overlap were documented for technical replicates of HLA class I samples (24). However, mLNs were significantly different, with exclusive presentation of the intestine-expressed genes Dmbt1, Maoa, Cps1, Fmo5, and Apoc2 and the absence of the skin-expressed genes Sbsn and Dmkn, among others. These findings, which are corroborated by mRNA expression data of murine specimens (Fig. 2B) and immunohistochemical analysis of human specimens (http://www.proteinatlas.org), indicate that the MHCII peptidome of regional LNs reflects, at least in part, anatomical location. It was suggested that peptides might be presented by migratory DCs or by other APCs residing in LNs, which might access the peptides transported in lymph fluids (3, 25). Direct identification by MS may allow us to study peptide-presentation mechanisms, without limitation to model Ags (such as OVA). However, the MS-based identification of Ags presented by distinct cell populations requires the sorting of cells prior to peptidome analysis, which is complicated by the low number of cells that can be recovered after such a procedure. The study of the MHC peptidome of different cell populations from in vivo–derived material naturally represents the next challenge in MHC peptidome analysis.

Table III. Bacterial peptide sequences identified with high confidence from healthy (M1–M2) or inflamed (C1–C5) mLNs

Peptide Sequence	PSMs	UniProt Accession	Modifications	*q* Value[a]	PEP	XCorr M1	XCorr M2	XCorr C1	XCorr C2	XCorr C3	XCorr C4	XCorr C5	Matrix-Based Score[b]
TQLLPLLPQ	3	N1ZXV2		0.002	0.0591	2.9							−14.782
ISERLDTIESI	1	N2A3B7		0.007	0.1623			2.8					−7.491
SSYANAEDMLTLTSH	2	N2A3Y1	M9 (Oxidation)	0.006	0.1957		2.2					2.7	0.730
EDEPTIREVLKEYMT	1	N2A8C1		0.003	0.1105		2.4						7.198
DILLMHCMTDGNWPETRKFY	1	UPI0002918219[c]	M8 (Oxidation)	0.006	0.0734					2.0			−4.746

Potential I-A^b binding sites are underlined.
[a] *q*-Value, FDR calculated with percolator.
[b] Matrix-based binding prediction score. A score > 8.5 predicted binding to I-A^b.
[c] UniParc accession number.
PEP, posterior error probability; PSM, peptide to spectrum match; XCorr, SEQUEST XCorr value.

To further validate that the peptide sequences identified from C57BL/6 LNs could bind to the cognate MHCII allele (I-A^b), we established a motif-based peptide binding prediction algorithm (Fig. 3, Supplemental Fig. 1A, 1B). This algorithm was based on previously published I-A^b– and I-A^d–specific motifs (7) and allowed us to predict the binding of 76.6–87.3% of peptide sequences from various biological sources to the cognate alleles, whereas only 7.8–19.6% of peptide sequences were predicted to bind to the unrelated allele. With the ability to discriminate between I-A^b–eluted peptides and peptides derived from other sources, it was possible to prove that 1% FDR represents the filter leading to MHCII peptidomes of very high quality (Supplemental Fig. 1C, 1D).

A comparative analysis of the MHCII peptidomes of healthy mice and animals with colitis revealed changes during inflammation. Prominent proteins identified exclusively or with significantly more peptides from inflamed LNs include Igs, such as IgA (Igha) and IgE (Ig ε chain C region), Bank1, Chpf, Cmip, Fth1, Slamf6, Tlr9, Itgb7, and Notch3 (Table II). B cells control intestinal microbiota through secretion of IgA, which was identified with a greater number of peptides during colitis. Moreover, some specific IgG sequences (e.g., protein Igkv4-61 and IgH V region 914) were identified exclusively during colitis, indicating clonal expansion of certain Ag-specific cells. It is possible that some of the IgG sequences are derived from the capture Ab, a rat IgG2b of unknown sequence. Further, IgE-derived peptides were identified exclusively during disease, which is in line with reports demonstrating that, in the murine T cell–transfer model, B cells producing IgE mediated oxazolone-induced colitis (26) and that an anti-IgE Ab ameliorated symptoms of DSS-induced colitis (27).

Other proteins presented exclusively during colitis include Notch3 (28), Slamf6 (29), and Bank1, which is involved in BCR signaling but also was recently found to control CpG-induced IL-6 secretion, in which Tlr9 is also involved (30). Identification of Chpf in LNs from mice with colitis was of interest, because oral administration of the protein was reported to ameliorate symptoms of DSS-induced colitis in rats (31). Together, these data suggest that many of the proteins, whose peptides are presented exclusively in inflamed mLNs, are involved in the immune response against pathogens or in the pathogenesis of colitis.

The intestinal immune system maintains a delicate balance between defense against pathogens and tolerance of commensal bacteria; an aberrant immune response against the latter may eventually lead to chronic colitis. Therefore, we searched the MS data against a database with the proteomes of eight bacterial strains contained in the altered Schaedler flora, which are widely used to inoculate germ-free founder animal breeding colonies (22). Of the 2188 peptides identified from healthy or inflamed mLNs, only five peptides were annotated unambiguously to bacterial proteins (Table III). Similar results were obtained with a database including all bacterial proteomes from UniProt (data not shown). However, the performance of very large databases in MHC peptidomics experiments is suboptimal as the increased search space negatively impacts statistical analysis. Our results indicate that the level of presentation of bacterial peptides in mLNs may be low. The main limitation of a proteomic investigation of peptides of bacterial origin relates to the heterogeneous nature of commensals and to the incomplete knowledge of their genomes. In most cases, 16S sequencing is performed to characterize intestinal bacteria, but this information is not sufficient for proteomic investigations (32). In the future, proteomic studies of germ-free animals inoculated with one or more sequenced bacterial strains would be desirable, to better characterize whether bacterial peptides are indeed presented in mLNs.

In summary, we described the purification of MHCII molecules from pools of six LNs, which led to the high-confidence identification of >1000 peptides on average. We applied this methodology to the study of the MHCII peptidome of aLNs, bLNs, iLNs, and mLNs, demonstrating the presence of skin and intestine-specific proteins, respectively. We also investigated the MHCII peptidome of mLNs during DSS-induced colitis, which revealed changes associated with the inflammatory process. It was reported that the abundance of an autoantigen is significantly increased in LNs of mice with destructive gastritis (3). Thus, the MS-based detection of specific peptides in regional LNs, combined with knowledge about protein function and tissue distribution, should facilitate the discovery of autoantigens in chronic inflammatory and autoimmune conditions.

Acknowledgments

We thank Prof. Cornelia Halin Winter, Dr. Erica Russo, and Martina Vranova (ETH Zurich) for scientific advice and technical support.

Disclosures

D.N. is a cofounder, shareholder, and member of the board of Philogen. T.F. and D.R. are employees of Philochem. The other authors have no financial conflicts of interest.

References

1. Buettner, M., and U. Bode. 2012. Lymph node dissection–understanding the immunological function of lymph nodes. *Clin. Exp. Immunol.* 169: 205–212.
2. Turley, S. J., A. L. Fletcher, and K. G. Elpek. 2010. The stromal and haematopoietic antigen-presenting cells that reside in secondary lymphoid organs. *Nat. Rev. Immunol.* 10: 813–825.
3. Scheinecker, C., R. McHugh, E. M. Shevach, and R. N. Germain. 2002. Constitutive presentation of a natural tissue autoantigen exclusively by dendritic cells in the draining lymph node. *J. Exp. Med.* 196: 1079–1090.
4. Hunt, D. F., H. Michel, T. A. Dickinson, J. Shabanowitz, A. L. Cox, K. Sakaguchi, E. Appella, H. M. Grey, and A. Sette. 1992. Peptides presented to the immune system by the murine class II major histocompatibility complex molecule I-Ad. *Science* 256: 1817–1820.
5. Bozzacco, L., H. Yu, H. A. Zebroski, J. Dengjel, H. Deng, S. Mojsov, and R. M. Steinman. 2011. Mass spectrometry analysis and quantitation of peptides presented on the MHC II molecules of mouse spleen dendritic cells. *J. Proteome Res.* 10: 5016–5030.
6. Suri, A., J. J. Walters, O. Kanagawa, M. L. Gross, and E. R. Unanue. 2003. Specificity of peptide selection by antigen-presenting cells homozygous or heterozygous for expression of class II MHC molecules: the lack of competition. *Proc. Natl. Acad. Sci. USA* 100: 5330–5335.
7. Sofron, A., D. Ritz, D. Neri, and T. Fugmann. 2016. High-resolution analysis of the murine MHC class II immunopeptidome. *Eur. J. Immunol.* 46: 319–328.
8. Caron, E., D. J. Kowalewski, C. Chiek Koh, T. Sturm, H. Schuster, and R. Aebersold. 2015. Analysis of major histocompatibility complex (MHC) immunopeptidomes using mass spectrometry. *Mol. Cell. Proteomics* 14: 3105–3117.
9. Bootz, F., B. Ziffels, and D. Neri. 2016. Antibody-based targeted delivery of interleukin-22 promotes rapid clinical recovery in mice with DSS-induced colitis. *Inflamm. Bowel Dis.* 22: 2098–2105.
10. Fugmann, T., D. Neri, and C. Roesli. 2010. DeepQuanTR: MALDI-MS-based label-free quantification of proteins in complex biological samples. *Proteomics* 10: 2631–2643.
11. Andreatta, M., O. Lund, and M. Nielsen. 2013. Simultaneous alignment and clustering of peptide data using a Gibbs sampling approach. *Bioinformatics* 29: 8–14.
12. Thomsen, M. C., and M. Nielsen. 2012. Seq2Logo: a method for construction and visualization of amino acid binding motifs and sequence profiles including sequence weighting, pseudo counts and two-sided representation of amino acid enrichment and depletion. *Nucleic Acids Res.* 40: W281–W287.
13. Lattin, J. E., K. Schroder, A. I. Su, J. R. Walker, J. Zhang, T. Wiltshire, K. Saijo, C. K. Glass, D. A. Hume, S. Kellie, and M. J. Sweet. 2008. Expression analysis of G protein–coupled receptors in mouse macrophages. *Immunome Res.* 4: 5.
14. Wu, C., I. Macleod, and A. I. Su. 2013. BioGPS and MyGene.info: organizing online, gene-centric information. *Nucleic Acids Res.* 41: D561–D565.
15. Andreatta, M., E. Karosiene, M. Rasmussen, A. Stryhn, S. Buus, and M. Nielsen. 2015. Accurate pan-specific prediction of peptide-MHC class II binding affinity with improved binding core identification. *Immunogenetics* 67: 641–650.
16. Germain, R. N., A. Bhattacharya, M. E. Dorf, and T. A. Springer. 1982. A single monoclonal anti-Ia antibody inhibits antigen-specific T cell proliferation controlled by distinct Ir genes mapping in different H-2 I subregions. *J. Immunol.* 128: 1409–1413.
17. Zhu, Y., A. Y. Rudensky, A. L. Corper, L. Teyton, and I. A. Wilson. 2003. Crystal structure of MHC class II I-Ab in complex with a human CLIP peptide: prediction of an I-Ab peptide-binding motif. *J. Mol. Biol.* 326: 1157–1174.
18. Nielsen, M., and O. Lund. 2009. NN-align. An artificial neural network-based alignment algorithm for MHC class II peptide binding prediction. *BMC Bioinformatics* 10: 296.
19. Wirtz, S., and M. F. Neurath. 2007. Mouse models of inflammatory bowel disease. *Adv. Drug Deliv. Rev.* 59: 1073–1083.
20. de Souza, H. S., and C. Fiocchi. 2016. Immunopathogenesis of IBD: current state of the art. *Nat. Rev. Gastroenterol. Hepatol.* 13: 13–27.
21. Coombes, J. L., and F. Powrie. 2008. Dendritic cells in intestinal immune regulation. *Nat. Rev. Immunol.* 8: 435–446.
22. Dewhirst, F. E., C. C. Chien, B. J. Paster, R. L. Ericson, R. P. Orcutt, D. B. Schauer, and J. G. Fox. 1999. Phylogeny of the defined murine microbiota: altered Schaedler flora. *Appl. Environ. Microbiol.* 65: 3287–3292.
23. Shao, S., T. Guo, V. Gross, A. Lazarev, C. C. Koh, S. Gillessen, M. Joerger, W. Jochum, and R. Aebersold. 2016. Reproducible tissue homogenization and protein extraction for quantitative proteomics using MicroPestle-assisted pressure-cycling technology. *J. Proteome Res.* 15: 1821–1829.
24. Caron, E., L. Espona, D. J. Kowalewski, H. Schuster, N. Ternette, A. Alpízar, R. B. Schittenhelm, S. H. Ramarathinam, C. S. Lindestam Arlehamn, C. Chiek Koh, et al. 2015. An open-source computational and data resource to analyze digital maps of immunopeptidomes. *eLife* 4: e07661.
25. Stern, L. J., and L. Santambrogio. 2016. The melting pot of the MHC II peptidome. *Curr. Opin. Immunol.* 40: 70–77.
26. Hoving, J. C., F. Kirstein, N. E. Nieuwenhuizen, L. C. Fick, E. Hobeika, M. Reth, and F. Brombacher. 2012. B cells that produce immunoglobulin E mediate colitis in BALB/c mice. *Gastroenterology* 142: 96–108.
27. Kang, O. H., D. K. Kim, Y. A. Choi, H. J. Park, J. Tae, C. S. Kang, S. C. Choi, Y. H. Nah, H. K. Lee, and Y. M. Lee. 2006. Suppressive effect of non-anaphylactogenic anti-IgE antibody on the development of dextran sulfate sodium-induced colitis. *Int. J. Mol. Med.* 18: 893–899.
28. Sansone, P., G. Storci, S. Tavolari, T. Guarnieri, C. Giovannini, M. Taffurelli, C. Ceccarelli, D. Santini, P. Paterini, K. B. Marcu, et al. 2007. IL-6 triggers malignant features in mammospheres from human ductal breast carcinoma and normal mammary gland. *J. Clin. Invest.* 117: 3988–4002.
29. van Driel, B., G. Wang, G. Liao, P. J. Halibozek, M. Keszei, M. S. O'Keeffe, A. K. Bhan, N. Wang, and C. Terhorst. 2015. The cell surface receptor Slamf6 modulates innate immune responses during *Citrobacter rodentium*–induced colitis. *Int. Immunol.* 27: 447–457.
30. Wu, Y. Y., R. Kumar, M. S. Haque, C. Castillejo-López, and M. E. Alarcón-Riquelme. 2013. BANK1 controls CpG-induced IL-6 secretion via a p38 and MNK1/2/eIF4E translation initiation pathway. *J. Immunol.* 191: 6110–6116.
31. Hori, Y., J. Hoshino, C. Yamazaki, T. Sekiguchi, S. Miyauchi, and K. Horie. 2001. Effects of chondroitin sulfate on colitis induced by dextran sulfate sodium in rats. *Jpn. J. Pharmacol.* 85: 155–160.
32. Nguyen, T. L., S. Vieira-Silva, A. Liston, and J. Raes. 2015. How informative is the mouse for human gut microbiota research? *Dis. Model. Mech.* 8: 1–16.